

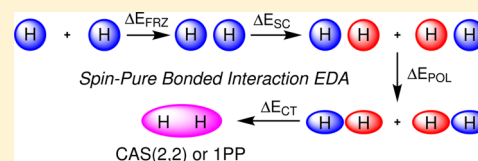
# Variational Energy Decomposition Analysis of Chemical Bonding. 1. Spin-Pure Analysis of Single Bonds

Daniel S. Levine, Paul R. Horn, Yuezhi Mao, and Martin Head-Gordon\*

Kenneth S. Pitzer Center for Theoretical Chemistry, Department of Chemistry, University of California, Berkeley, California 94720, United States

Chemical Sciences Division, Lawrence Berkeley National Laboratory, Berkeley, California 94720, United States

**ABSTRACT:** We have designed an energy decomposition analysis (EDA) to gain a deeper understanding of single chemical bonds, that is, those in which the interacting fragments are doublet open-shell systems but the supersystem is closed-shell. The method is a spin-pure extension of the absolutely localized molecular orbital (ALMO) EDA to the one-pair perfect pairing energy (equivalently to an active space of two electrons in two orbitals). The total interaction energy is broken up into four terms: frozen interactions, spin-coupling, polarization, and charge-transfer. A variety of single bonds are analyzed and, in addition, we use this method to show how solvation changes the nature of bonds, producing different results in the gas-phase and with explicit solvent molecules.



## 1. INTRODUCTION

Practical chemistry relies on the qualitative application of physical and chemical principles (e.g., electrostatics, polarizability, electronegativity, etc.) to understand the interaction of molecules when investigating the synthesis and reactivity of molecular systems. Theoretical chemistry, on the other hand, does away with these principles in favor of a quantitative quantum mechanical treatment with no specific appeal to any of these ideas. The success of the former approach suggests that there is value in thinking about chemistry in the context of these heuristics. At the heart of the matter is the question: What is the nature of the chemical bond.<sup>1–3</sup>

Since the advent of quantum mechanics, there has been over 80 years of work on this problem, which we shall attempt to very briefly summarize. At the level of the role of different terms in the Hamiltonian, there were originally two possibilities that could explain the origin of the stability of the covalent bond. Since chemical bonding in elementary systems such as the one-electron bond in  $H_2^+$  is associated with an increase in electron density in the bonding region, it was suggested<sup>4</sup> that this was electrostatically favored (i.e., lowered the potential energy). However, detailed analysis has supported the competing possibility that delocalization of previously localized electrons in the molecule in fact lowers the kinetic energy and that this is the principal origin of stabilization in covalent bonds. This result has been established for simple systems by Ruedenberg and co-workers,<sup>2,5</sup> Kutzelnigg,<sup>6</sup> and others.<sup>7–9</sup> Ruedenberg et al.<sup>10</sup> as well as others<sup>11–13</sup> have also reported progress toward extracting similar information from more complex molecules.

Numerous other methods have also been developed to analyze chemical bonds, from a variety of complementary perspectives. One of the most widely used is Weinhold et al. Natural Bond Orbital (NBO) analysis,<sup>14</sup> which yields localized orbitals, information on hybridization, chemical bonds, atomic

charges, and predominant Lewis structures. Topological analysis of the electron density, as developed in the quantum theory of atoms-in-molecules (QTAIM),<sup>15</sup> is another well-developed method for diagnosing the presence of chemical bonds (via so-called bond critical points), as well as partitioning an energy into intra-atomic and interatomic terms. Other topological methods involve increasingly complicated functions of the density and the kinetic energy density, of which the electron localization function (ELF) is a prominent example. A variety of other methods exist for partitioning a bond energy into sums of terms that are physically interpretable.<sup>16,17</sup>

At the same time, much progress has been made in analyzing nonbonded interactions into contributions that include dispersion, permanent and induced electrostatics which are well-defined in the nonoverlapping regime, as well as Pauli repulsion and charge transfer. These schemes include perturbative methods such as the Symmetry Adapted Perturbation Theory (SAPT)<sup>18–25</sup> method and Natural Energy Decomposition Analysis (NEDA)<sup>26–28</sup> and methods based on variationally optimized, constrained, intermediate wave functions, such as Kitaura and Morokuma (KM) EDA,<sup>29</sup> the Ziegler-Rauk approach for the  $X\alpha$  method,<sup>30–32</sup> and the Block-Localized Wave function (BLW-EDA)<sup>33,34</sup> of Mo and Gao and the related Absolutely Localized Molecular Orbital (ALMO-EDA) of Head-Gordon et al.<sup>35–40</sup> Such energy decomposition analysis (EDA) schemes have had considerable success at describing the interactions of closed-shell fragments as well as open-shell–closed-shell interactions.<sup>41–43</sup>

A number of the general EDA schemes mentioned for nonbonded interactions above have been applied to bonded interactions.<sup>30–32,44,45</sup> These schemes usually group all of the terms assignable to the bond (polarization, charge-transfer, etc.)

Received: June 3, 2016

Published: August 29, 2016

into a single orbital interactions term, possibly separable into different wave function symmetries (e.g.,  $\sigma$ ,  $\pi$  bonding).<sup>46</sup> We are interested in developing methods specifically for the variational energy decomposition analysis of chemical bonds relative to radical fragments. Motivated by earlier work in our group on the ALMO-EDA for nonbonded interactions, the objective is to define a sequence of constraints which can be ascribed to deletion of specific physical effects, such as charge transfer, polarization, and spin coupling. Our perspective of a sequence of progressively weaker variational constraints contrasts with energy partitioning methods that do not define optimized intermediate states.

This paper reports the design and implementation of an EDA for single bonds, the simplest case. The homolytic separation of a single bond into two doublet radical fragments cannot be accomplished in a spin-pure way using single determinant theory. The simplest spin-pure wave function involves recoupling two electrons in two orbitals, which is variously known as CAS(2,2),<sup>47</sup> one-pair perfect pairing,<sup>48</sup> and two-configuration SCF.<sup>49</sup> The EDA reported here defines a sequence of constraints that yield three intermediate variational energies in addition to the final CAS(2,2) energy. A descriptive and nonmathematical discussion of the design principles is given in the following section on Design Principles, followed by the mathematical framework which enables the constraints to be exactly satisfied. After mentioning some computational details, we present results and discussion for a variety of single bonds, whose characters vary considerably, including some consideration of the effect of solvation.

## 2. DESIGN PRINCIPLES

Our objective is to construct a bonded energy decomposition analysis that adheres to the following criteria (these are the essential parts of a longer list one of us suggested for a nonbonded EDA<sup>37</sup>): 1) all energies should be calculated using valid Fermionic wave functions, 2) all such wave functions should be spin-pure, 3) the method should qualitatively correctly describe the interaction over the entire potential energy surface, and 4) the method should be variational with respect to a well-defined total interaction energy.

In this work, the absolutely localized molecular orbital (ALMO) EDA is extended to accomplish these goals by decomposing the one-pair perfect pairing (PP1) energy (or, equivalently, the CAS(2,2) energy). Two (nonorthogonal) fragments are defined as the two halves of the bond of interest, and the orbitals are optimized in isolation as restricted open-shell fragments. These fragments are then brought together with frozen orbitals to form a high-spin supersystem (giving rise to a frozen orbital term, FRZ). The unpaired electrons in this supersystem are then used to generate the singlet configuration state function, in which the ALMO constraint prevents charge-transfer between the fragments (giving a term due to spin-coupling of the bond electrons, SC). This CSF is allowed to relax subject to the CT-preventing ALMO constraint (giving a polarization term, POL). Finally, the ALMO constraint is relaxed to give the one-pair perfect pairing solution (giving a term assignable to charge-transfer, CT).

We therefore partition the single bonded interaction of interest into five terms:

$$\Delta E_{\text{interaction}} = \Delta E_{\text{GEOM}} + \Delta E_{\text{FRZ}} + \Delta E_{\text{SC}} + \Delta E_{\text{POL}} + \Delta E_{\text{CT}} \quad (1)$$

The first term,  $\Delta E_{\text{GEOM}}$ , is the energy penalty associated with distorting each radical fragment to the geometry it adopts in the interacting complex. Each radical fragment is described by a spin-pure ( $S = \frac{1}{2}$ ;  $M_S = +\frac{1}{2}$ ) single determinant (i.e., restricted open shell Hartree–Fock).

The second term,  $\Delta E_{\text{FRZ}}$ , is the energy change associated with bringing the two radical fragments together from infinite separation to form a spin-pure triplet single determinant wave function ( $S = 1$ ;  $M_S = +1$ ). The triplet wave function is constructed without allowing the orbitals to relax. By design,  $\Delta E_{\text{FRZ}}$  is entirely a nonbonded interaction, and for this reason will typically be repulsive for a chemical bond. It includes contributions from interfragment electrostatics, Pauli repulsion, exchange-correlation, and dispersion (although dispersion is not present in the current implementation since it is based on Hartree–Fock theory). Being analogously defined to the existing ALMO frozen term, it may be decomposed into those contributions if desired using the ALMO frozen decomposition scheme.<sup>38,39</sup>

The third term,  $\Delta E_{\text{SC}}$ , is the only term that has no analog in the ALMO-EDA for nonbonded interactions and is the energy difference due to changing the coupling of the two radical electrons from high-spin triplet to low-spin singlet. It accounts for the delocalization effects associated with singlet coupling of two electrons forming the single bond, while continuing to use the frozen orbitals.  $\Delta E_{\text{SC}}$  is expected to often be a dominant term in covalent bond formation.

The fourth term,  $\Delta E_{\text{POL}}$ , is the energy change associated with the orbitals of each fragment relaxing in the presence of the field of the other fragment, without any charge transfer, subject to singlet spin coupling.  $\Delta E_{\text{POL}}$  includes contributions from polarization in the bond. The original atomic-orbital based ALMO-EDA polarization term does not have a well-defined basis set limit;<sup>50</sup> as the basis set gets larger, there is sufficient flexibility that orbitals can contort to approximate the final wave function, including charge-transfer. The use of fragment electric response functions (FERFs) as an alternative ALMO basis resolves this issue.<sup>37,40</sup> In this scheme, the virtual orbitals available for polarization are only those which are necessary for describing the response of each fragment to an applied electric field. We will use the dipole and quadrupole (DQ) FERFs to define the fragment virtual spaces within which the polarization energy is minimized. This guarantees a well-defined basis set limit: the polarization term describes how much the fragments relax due to the dipole–quadrupole field generated by the other fragments.

The final term,  $\Delta E_{\text{CT}}$ , contains charge-transfer contributions relating to electrons from one fragment being transferred to the other fragment. It is clearly the dominant term in ionic bonds and is also expected to be important in bonds of the so-called charge-shift type.<sup>51–53</sup>

## 3. THEORY

We employ the tensor formulation for working with non-orthogonal orbitals<sup>54</sup> and use the following notation in this work: total wave function:  $\Psi$ ; Slater determinant:  $\phi$ ; determinant indices: boldface letters  $\mathcal{A}$ ,  $\mathcal{B}$ , and  $\mathcal{C}$ ; fragment indices: capital Roman  $X$ ,  $Y$ ,...; AO indices: lower case Greek  $\mu, \nu$ ,...; occupied MO indices:  $i, j$ ,...; generic MO indices  $r, s$ ,... Large dots are used as placeholders to clarify index ordering. Covariant indices are given as subscripts and contravariant indices as superscripts.

**3.1. Frozen Energy.** For readers unfamiliar with the ALMO scheme,<sup>35,36,40</sup> we outline the method below. The system of interest is partitioned into some number of interacting fragments (in this case, the two sides of the bond of interest). Separate restricted open-shell single-point calculations are performed on each of the fragments in isolation (at the geometry of interacting system). The resulting fragment MO coefficients are assembled into a high-spin (triplet for a single-bond), unrestricted supersystem MO coefficient matrix by block-diagonal concatenation. The orbitals are thus said to be absolutely localized on a given fragment. Note that, while orbitals within a fragment are orthogonal, between fragments, this is generally not the case. The supersystem wave function is still spin-pure because the fragment blocks are restricted open-shell and are high-spin coupled.

The concatenated MO coefficients of the supersystem give rise to a supersystem “frozen” density matrix,  $P_{\text{FRZ}}$ , for both alpha and beta spins, defined by the subspace spanned by the frozen occupied orbitals

$$P_{\alpha, \text{FRZ}}^{X\mu Y\nu} = (T_{\alpha, \text{FRZ}})_{\bullet X\mu}^{X\mu} (\sigma_{\alpha})^{X\mu Y\nu} (T_{\alpha, \text{FRZ}})_{\bullet Y\nu}^{Y\nu} \quad (2)$$

where  $(\sigma_{\alpha})^{X\mu Y\nu}$  is the contravariant alpha occupied MO metric and is needed to form a valid projector. This matrix is identity only when the fragments are orthogonal and there is no overlap between them. Hence, in general, the frozen density is not the sum of the noninteracting densities. The contravariant alpha occupied MO metric is the inverse of the occupied-occupied block of the covariant alpha MO overlap matrix,  $(\sigma_{\alpha})_{X\mu Y\nu}$

$$(\sigma_{\alpha})_{X\mu Y\nu} = (T_{\alpha})_{\bullet X\mu}^{X\mu} S_{X\mu Y\nu} (T_{\alpha})_{\bullet Y\nu}^{Y\nu} \quad (3)$$

where  $S_{X\mu Y\nu}$  is the covariant atomic orbital overlap matrix. We then calculate the frozen contribution by the difference between the sum of single point energies for the separated fragments and the energy of the supersystem, that is, the trace of the frozen density with the supersystem core Hamiltonian and Fock matrices, formed from the frozen density:

$$E_{\text{FRZ}} = \frac{1}{2} \text{tr}[(H_{\text{core}} + F_{\alpha, \text{FRZ}})P_{\alpha, \text{FRZ}} + (H_{\text{core}} + F_{\beta, \text{FRZ}})P_{\beta, \text{FRZ}}] \quad (4)$$

$$\Delta E_{\text{FRZ}} = E_{\text{FRZ}} - \sum_Z^{\text{Frgm}} E_Z \quad (5)$$

In highly symmetric systems, the unpaired spin-orbital on each fragment resides in a degenerate energy eigenspace, and so there are many degenerate solutions for the fragments (see Figure 1). While these different solutions may be degenerate for the fragments, the supersystems assembled from these different fragments solutions are not, in general, degenerate. To resolve this ambiguity, the initially formed high-spin supersystem energy is spin-flipped to a spin-coupled wave function (see the following sections), which is optimized with respect to orbital rotations subject to the ALMO constraint. These polarized fragments are then used as the initial guess for new fragment calculations which are minimized, subsequently, with respect to doubly occupied-virtual orbital rotations, singly occupied-virtual rotations, and finally all orbital rotations. We thus obtain unpolarized fragments that have had their spins reoriented to be consistently and appropriately aligned for bonding. The stepwise relaxation procedure is to ensure that the polarized fragments unpolarize without the singly occupied orbital rotating away from the correct (that is, energetically optimal)

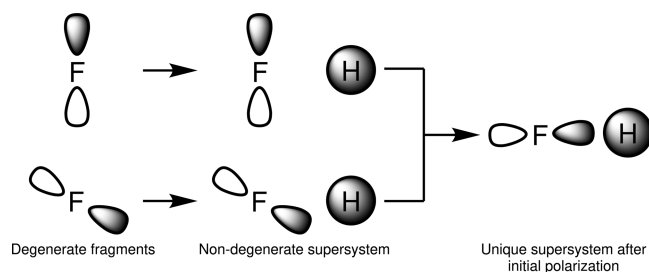


**Figure 1.** An example of a case where there are many degenerate solutions for the fragments (the F atom) but the assembled supersystem (HF) is not necessarily degenerate. The unpaired spin-orbital is shown. To form a unique supersystem, the singlet-coupled supersystem energy is optimized with respect to orbital rotations, and then the polarized fragments form the initial guess for relaxation back to the correctly oriented ground state.

orientation. These unpolarized fragments are then used to construct the true frozen supersystem wave function.

In principal, this reorientation and unpolarization procedure could result in fragments in a low-lying electronic excited state. We therefore define an electronic distortion energy analogous to the geometric distortion energy, as the energy difference between the fragments in the lowest electronic state and the fragments in the electronic state of the interacting complex. Generally, and in all cases so far studied, this term is zero, but it can, in principle, be positive. The energy change from not resolving this orientational ambiguity can be substantial. For example, for the HF molecule, the frozen terms due to different singly occupied orientations (of the F atom) can be different by >50 kcal/mol.

Since this method is an extension of the ALMO EDA scheme, it inherits the ALMO scheme's ability to further separate the frozen term into terms corresponding to permanent electrostatic interactions, Pauli repulsion, and dispersion.<sup>39</sup>

**3.2. Spin-Coupling.** In order to generate the singlet CSF from the triplet frozen supersystem wave function, a spin flip is applied to each of the unpaired electrons in each fragment space to form a 2-configurational wave function. Since the two determinants that make up the CSF are spin complements, the CI coefficients are equal

$$|\Psi_{\text{SC}}\rangle = N(|\phi_{\mathcal{A}}\rangle + |\phi_{\mathcal{B}}\rangle) \quad (6)$$

where  $N$  is a normalization factor. The spin-coupling energy is then calculated as the energy difference between the frozen supersystem energy and the energy of the 2-configurational wave function:

$$E_{\text{SC}} = N^2(E_{\mathcal{A}} + E_{\mathcal{B}} + 2E_{\mathcal{AB}}) \quad (7)$$

$$\Delta E_{\text{SC}} = E_{\text{SC}} - E_{\text{FRZ}} \quad (8)$$

This energy change may be positive or negative depending on which of the triplet or the singlet is lower in energy. Generally, if a bond is forming, the singlet will be lower in energy and the energy change is negative.

**3.3. Polarization.** In order to calculate the variational polarization energy subject to the ALMO constraint while ensuring spin-purity, we require each fragment to continue to be described by a set of restricted open-shell orbitals. The spin-coupled determinants are already ALMO wave functions due to the block-diagonal nature of the MO coefficients matrix; the



ALMO constraint is maintained by only allowing rotations within a fragment. In this section, we derive expressions for the gradient of the energy with respect to nonorthogonal orbital rotations within each determinant and also for the interdeterminantal Hamiltonian matrix element.

Recall that the energy of the 2-configurational wave function is given by  $E = N^2(E_{\mathcal{A}} + E_{\mathcal{B}} + 2E_{\mathcal{AB}})$ . Ignoring normalization and differentiating with respect to an orbital rotation in arbitrary determinant  $\mathcal{C}$

$$\frac{\partial E}{\partial \Delta_{\mathcal{C}p\mathcal{C}q}} = \frac{\partial E_{\mathcal{A}}}{\partial \Delta_{\mathcal{C}p\mathcal{C}q}} + \frac{\partial E_{\mathcal{B}}}{\partial \Delta_{\mathcal{C}p\mathcal{C}q}} + 2 \frac{\partial E_{\mathcal{AB}}}{\partial \Delta_{\mathcal{C}p\mathcal{C}q}} \quad (9)$$

We first calculate the gradient within each determinant, that is, the first two terms (the determinant indices will be temporarily elided since they are all the same in this case). The energy of each determinant is given by

$$\frac{1}{2} \text{tr}[(\mathbf{H}_{\text{core}} + \mathbf{F}_{\alpha})\mathbf{P}_{\alpha} + (\mathbf{H}_{\text{core}} + \mathbf{F}_{\beta})\mathbf{P}_{\beta}] \quad (10)$$

We denote an orbital rotation between orbital  $p$  and  $q$  in fragment  $Z$  by  $\Delta_{Zp,Zq}$ . Then,

$$\frac{\partial E_{\mathcal{A}}}{\partial \Delta_{Zp,Zq}} = (F_{\alpha})_{B\mu A\mu} \frac{\partial (P_{\alpha})^{A\mu B\mu}}{\partial \Delta_{Zp,Zq}} + (F_{\beta})_{B\mu A\mu} \frac{\partial (P_{\beta})^{A\mu B\mu}}{\partial \Delta_{Zp,Zq}} \quad (11)$$

The required partial derivatives are

$$\frac{\partial P^{A\mu B\mu}}{\partial \Delta_{Zp,Zq}} = T_{\bullet A\mu}^{\bullet} (\sigma)^{A\mu B\mu} \frac{\partial T_{\bullet B\mu}^{\bullet}}{\partial \Delta_{Zp,Zq}} + T_{\bullet A\mu}^{\bullet} (\sigma)^{A\mu B\mu} \frac{\partial T_{\bullet B\mu}^{\bullet}}{\partial \Delta_{Zp,Zq}} + \frac{\partial T_{\bullet A\mu}^{\bullet}}{\partial \Delta_{Zp,Zq}} (\sigma)^{A\mu B\mu} T_{\bullet B\mu}^{\bullet} \quad (12)$$

$$= T_{\bullet A\mu}^{\bullet} (\sigma)^{A\mu B\mu} C_{\bullet B\mu}^{\bullet} (\delta_{Zp}^{B\mu} \delta_{Zq}^{B\mu} - \delta_{Zq}^{B\mu} \delta_{Zp}^{B\mu}) - T_{\bullet A\mu}^{\bullet} (\sigma)^{A\mu B\mu} T_{\bullet B\mu}^{\bullet} \quad (13)$$

$$\frac{\partial (\sigma)^{A\mu B\mu}}{\partial \Delta_{Zp,Zq}} = - \sum_{X,Y}^{\text{Frgm}} (\sigma)^{A\mu B\mu} \left( \frac{\partial (\sigma)_{X\mu Y\mu}}{\partial \Delta_{Zp,Zq}} \right) (\sigma)^{Y\mu B\mu} \quad (14)$$

$$= - \sum_{X,Y}^{\text{Frgm}} [(\sigma)^{A\mu B\mu} C_{\bullet X\mu}^{\bullet} (\delta_{Zp}^{X\mu} \delta_{Zq}^{X\mu} - \delta_{Zq}^{X\mu} \delta_{Zp}^{X\mu}) S_{X\mu Y\mu}^{\bullet} T_{\bullet Y\mu}^{\bullet} (\sigma)^{Y\mu B\mu} + (\sigma)^{A\mu B\mu} T_{\bullet X\mu}^{\bullet} S_{X\mu Y\mu}^{\bullet} (\delta_{Zp}^{Y\mu} \delta_{Zq}^{Y\mu} - \delta_{Zq}^{Y\mu} \delta_{Zp}^{Y\mu}) (\sigma)^{Y\mu B\mu}] \quad (15)$$

Combining terms and contracting with  $F_{B\mu A\mu}$

$$F_{B\mu A\mu} \frac{\partial P^{A\mu B\mu}}{\partial \Delta_{Zp,Zq}} = C_{\bullet X\mu}^{\bullet} (1 - S_{X\mu Y\mu}^{\bullet} F_{Y\mu B\mu}^{\bullet}) F_{B\mu A\mu} T_{\bullet A\mu}^{\bullet} (\sigma)^{A\mu B\mu} (\delta_{Zp}^{X\mu} \delta_{Zq}^{X\mu} - \delta_{Zq}^{X\mu} \delta_{Zp}^{X\mu}) + (\sigma)^{Y\mu B\mu} T_{\bullet B\mu}^{\bullet} F_{B\mu A\mu} (1 - P^{A\mu X\mu} S_{X\mu Y\mu}^{\bullet}) \times C_{\bullet Y\mu}^{\bullet} (\delta_{Zp}^{Y\mu} \delta_{Zq}^{Y\mu} - \delta_{Zq}^{Y\mu} \delta_{Zp}^{Y\mu}) \quad (16)$$

Which gives the matrix equation

$$\frac{\partial E_{\mathcal{A}}}{\partial \Delta_{pq}} = 2\{[(\sigma_{\alpha}^{-1})^m T_{\alpha}^T F_{\alpha} (1 - P_{\alpha} S) C_t + (\sigma_{\beta}^{-1})^m T_{\beta}^T F_{\beta} \times (1 - P_{\beta} S) C_t](\delta_p^t \delta_q^m - \delta_q^t \delta_p^m)\}_{ZZ} \quad (17)$$

where the superscript  $m$  denotes rows of the occupied metric, and the subscript  $t$  denotes columns of the MO coefficient matrix.

The gradient for the interdeterminantal matrix element follows a similar derivation. We define  $D_{\mathcal{AB}}$ , the determinant of the overlap matrix between the two determinants,  $D_{\mathcal{AA}}$  and  $D_{\mathcal{BB}}$ , the determinants of each determinant's overlap matrix,  $F_{\mathcal{AB}}$ , the transition Fock matrix, and  $P^{\mathcal{B}\nu \mathcal{A}\mu}$ , the transition

density matrix, and  $g^{\mathcal{B}\mathcal{B}j\mathcal{A}i}$  is the inverse of the nonsymmetric interdeterminantal occupied MO metric (the interdeterminantal analog of  $\sigma$  above). Let  $U = 1/2(h_{\mathcal{A}\mu \mathcal{B}\nu} + F_{\mathcal{A}\mu \mathcal{B}\nu}) P^{\mathcal{B}\nu \mathcal{A}\mu}$ .

$$\frac{\partial E_{\mathcal{AB}}}{\partial \Delta_{\mathcal{C}p\mathcal{C}q}} = \frac{\partial D_{\mathcal{AB}} / (D_{\mathcal{AA}} D_{\mathcal{BB}})^{1/2} U}{\partial \Delta_{\mathcal{C}p\mathcal{C}q}} \quad (18)$$

$$= \frac{D_{\mathcal{AB}}}{(D_{\mathcal{AA}} D_{\mathcal{BB}})^{1/2}} F_{\mathcal{A}\mu \mathcal{B}\nu} \frac{\partial P^{\mathcal{B}\nu \mathcal{A}\mu}}{\partial \Delta_{\mathcal{C}p\mathcal{C}q}} + E_{\mathcal{AB}} g^{\mathcal{B}\mathcal{B}j\mathcal{A}i} \quad (19)$$

$$\frac{\partial g^{\mathcal{B}\mathcal{B}j\mathcal{A}i}}{\partial \Delta_{\mathcal{C}p\mathcal{C}q}} - \frac{1}{2} E_{\mathcal{AB}} \left( \sigma^{\mathcal{B}Cn, \mathcal{B}D0} \frac{\partial \sigma^{\mathcal{B}Cn, \mathcal{B}D0}}{\partial \Delta_{\mathcal{C}p\mathcal{C}q}} + \sigma^{\mathcal{A}Ev, \mathcal{A}Fw} \frac{\partial \sigma^{\mathcal{A}Ev, \mathcal{A}Fw}}{\partial \Delta_{\mathcal{C}p\mathcal{C}q}} \right)$$

$$P^{\mathcal{B}\mathcal{B}\nu, \mathcal{A}\mathcal{A}\mu} = T_{\bullet \mathcal{B}\mathcal{B}j}^{\bullet} (g^{\mathcal{B}\mathcal{B}j\mathcal{A}i}) T_{\bullet \mathcal{A}\mathcal{A}\mu}^{\bullet} \quad (20)$$

$$g^{\mathcal{B}\mathcal{B}j\mathcal{A}i} = [T_{\bullet \mathcal{A}\mathcal{A}i}^{\bullet} S_{\mathcal{A}\mathcal{A}j\mathcal{B}\mathcal{B}0} T_{\bullet \mathcal{B}\mathcal{B}j}^{\bullet}]^{-1} \quad (21)$$

Note that when  $\mathcal{A} = \mathcal{B}$ , this expression reduces to the on-determinantal result derived above. Without loss of generality, we assume that orbital rotations are in the  $\mathcal{B}$  determinant. The first term's derivation is nearly identical to the on-determinantal case and gives the matrix expression

$$\frac{D_{\mathcal{AB}}}{(D_{\mathcal{AA}} D_{\mathcal{BB}})^{1/2}} \{((g_{\alpha}^{-1})^l T_{\alpha}^T F_{\alpha} (1 - P_{\alpha} S) C_{\mathcal{B}s} + (g_{\beta}^{-1})^l T_{\beta}^T F_{\beta} (1 - P_{\beta} S) C_{\mathcal{B}s})(\delta_p^s \delta_q^l - \delta_q^s \delta_p^l)\}_{ZZ} \quad (22)$$

where the superscript  $l$  denotes rows of the occupied metric, and the subscript  $s$  denotes columns of the MO coefficient matrix. The second and third terms together give the matrix expression

$$E_{\mathcal{AB}} \{((g_{\alpha}^{-1})^i T_{\alpha}^T F_{\alpha} + (g_{\beta}^{-1})^i T_{\beta}^T F_{\beta} - (\sigma_{\beta}^{-1})^i T_{\beta}^T F_{\beta} - (\sigma_{\beta}^{-1})^i T_{\beta}^T F_{\beta}) S_{\mathcal{B}r} (\delta_p^r \delta_q^i - \delta_q^r \delta_p^i)\}_{ZZ} \quad (23)$$

where the superscript  $i$  denotes rows of the occupied metric, and the subscript  $r$  denotes columns of the MO coefficient matrix. When  $\mathcal{A} = \mathcal{B}$ , this expression is zero.

This gradient expression is used to generate a RO gradient expression, that is, doubly occupied-singly occupied rotations, doubly occupied-virtual rotations, and singly occupied-virtual rotation are all carried out independently. This maintains the RO nature of each fragment and, hence, spin-purity of the total wave function. The energy change (which must be negative) due to this orbital relaxation is defined as the polarization energy term.

It should also be observed that some of this polarization is "constant-density" polarization,<sup>38</sup> which relieves some Pauli-repulsion and may be thought of as a deficiency in the initially defined spin-coupled wave function. However, based on previous results, we neglect this relatively minor component of the polarization energy.

**3.4. Charge-Transfer.** The relaxation of the ALMO constraint on the above 2-configurational wave function is the one-pair perfect pairing energy or, equivalently, CAS(2,2). The energy difference between the unconstrained PP energy and the polarized wave function energy is always negative and attributed to charge-transfer, a process that is formally forbidden before due to the ALMO constraint. As a result, the EDA described in this paper is therefore equivalently

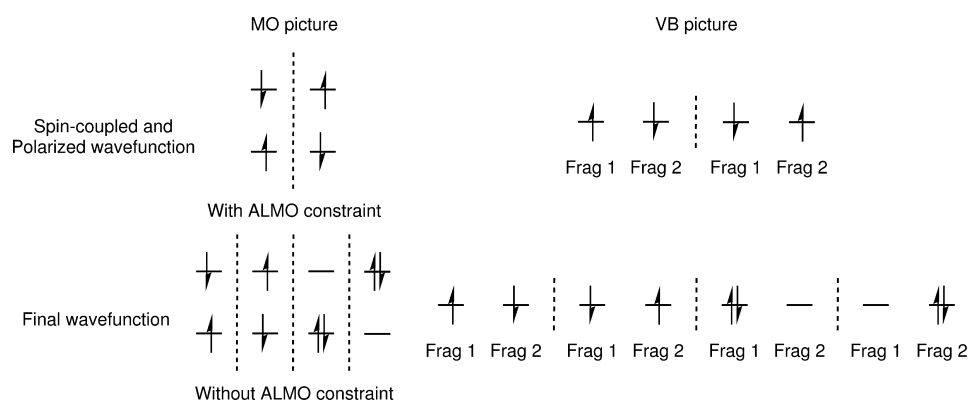


Figure 2. MO vs VB picture of EDA intermediate wave functions.

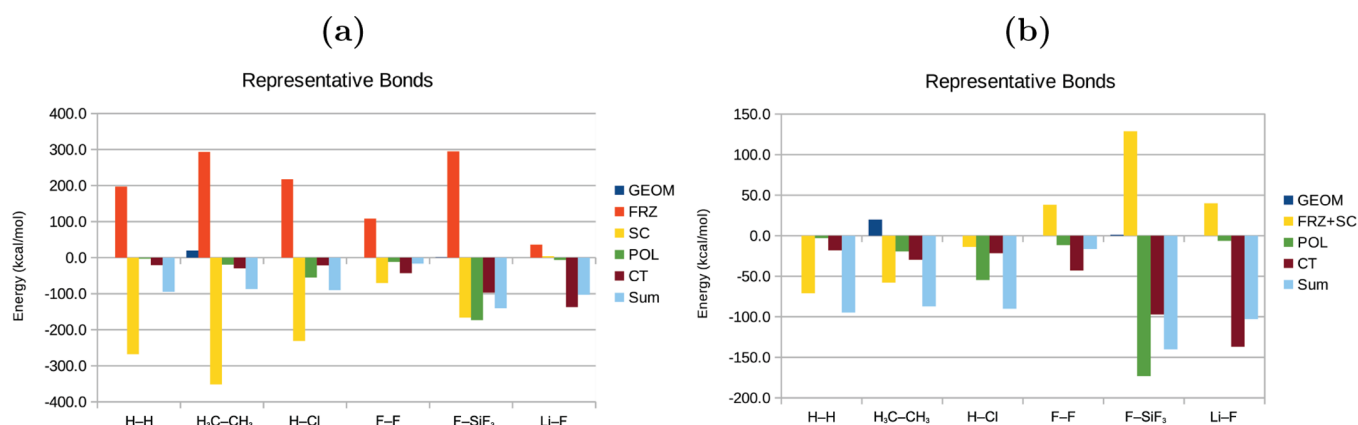


Figure 3. a) EDA of some representative bonds. b) EDA of some representative bonds with the frozen and spin-coupling terms summed.

Table 1. EDA of Representative Bonds<sup>a</sup>

	GEOM	FRZ	SC	POL	CT	sum	exact
H–H	0.0	196.9	–267.9	–2.9	–20.8	–94.7	–107.4
			(91.9)	(1.0)	(7.1)		
H <sub>3</sub> C–CH <sub>3</sub>	19.9	293.7	–351.6	–19.5	–29.6	–87.1	–91.4
			(87.8)	(4.9)	(7.4)		
H–Cl	0.0	217.2	–231.0	–54.7	–21.5	–90.0	–106.4
			(75.2)	(17.8)	(7.0)		
F–F	0.0	108.5	–70.3	–11.7	–42.9	–16.4	–30.4
			(56.3)	(9.4)	(34.4)		
F–SiF <sub>3</sub>	1.3	295.1	–166.3	–173.2	–97.1	–140.1	–166.0
			(38.1)	(39.7)	(22.2)		
Li–F	0.0	35.9	4.2	–6.3	–136.8	–103.0	–137.4
				(4.4)	(95.6)		

<sup>a</sup>All energies are in kcal/mol. Numbers in parentheses are the percentage of the total stabilizing interaction energy each term represents. Exact is CCSD(T)/aug-cc-pVTZ.

described as a PP-EDA or a CAS(2,2)-EDA. This final interaction energy is typically about 85% of the exact result, owing to the lack of dynamical correlation (*vide infra*).

#### 4. COMPUTATIONAL DETAILS

A development version of Q-Chem 4.3 was used for all calculations.<sup>55</sup> Geometries for each system were optimized at the HF/aug-cc-pVTZ level. The aug-cc-pVTZ basis was also used for all EDA calculations, which decompose the bond energy evaluated at the CAS(2,2) (equivalently 1-pair perfect pairing) level relative to ROHF fragments.

#### 5. RESULTS AND DISCUSSION

The EDA scheme introduced here is designed to follow the formation of a bond via a sequence of constrained variational calculations that bring together the two sides of the bond from infinite separation of the fragments. The initial supersystem wave function (from which the frozen energy term derives) corresponds to bringing together fragments with doublet-optimized orbitals in which no bond has formed. The spin-coupled wave function then represents the jump to the singlet surface and so reports on the singlet–triplet gap of the doublet-optimized orbitals. We argue that this energy difference then indicates how “covalent” a bond is, as covalency loosely

corresponds to the idea that electrons would rather be coupled than not coupled. The polarization term allows the orbitals to relax in the field of the other fragment, and hence large numbers correspond to how polar a bond is or, rather, how much energy is released by the density distorting to respond to the field of the other fragment. The final charge-transfer term corresponds to the energy stabilization due to charge flow between fragments. As one would expect, this term is dominant for ionic molecules but still plays an important, if smaller, role for classical covalent molecules.

Though this method is a MO-based method, it has clear connections to valence-bond descriptions of molecules. The ALMO-constrained, spin-coupled, and polarized wave functions, with their nonorthogonal interacting valence doublet fragments, are analogous to the valence-bond covalent picture (see Figure 2). The unconstrained, final wave function then corresponds to the 4-configurational extension of this VB wave function to include ionic terms in which both electrons of the bond lie on one fragment. Hence, the charge-transfer term in this method also includes what has been described as “charge-shift bonding”.<sup>51–53</sup>

To verify that the EDA behaves as expected, we investigated a few representative and pathological bonds (Figure 3 and Table 1). Classic, nonpolar covalent bonds such as H<sub>2</sub> and ethane are indeed dominated by spin-coupling. Polarization and charge transfer make up only a small portion of the interaction energy (bond energy). As we move to more polar bonds, as in HCl, polarization becomes highly important to the interaction in addition to spin-coupling, giving what we would call a typical polar covalent bond. Molecules which feature charge-transfer contributions that are similar in magnitude to the spin-coupling term are considered “charge-shift bonds”, as exemplified by F<sub>2</sub>, a canonical “charge-shift” bond. One of the strongest single bonds, the Si–F bond of SiF<sub>4</sub>, which has high spin-coupling, polarization, and charge-transfer, could be equivalently thought of as a polar covalent bond with ionic character or a polar charge-shift bond. When the bond is truly ionic, as in LiF, neither spin-coupling nor polarization is significant, and the bond energy is dominated by the charge transfer term. Hence, the consideration of the terms of this EDA gives a “fingerprint” for classical chemical concepts of bonding. This fingerprint was obtained without any explicit reference to these concepts, and the method gives a quantitative description of these qualitative chemical heuristics.

We can compare this EDA to other (broken-symmetry) schemes that have been used for bonded interactions, such as the Bickelhaupt-Baerends implementation of the Ziegler-Rauk EDA, in which the energy is decomposed into electrostatics, Pauli repulsion, and orbital response terms.<sup>56</sup> To compare this to ZR-EDA, we calculated the electrostatics and Pauli repulsion terms for the broken symmetry ethane and fluorine molecules and grouped them as a broken symmetry frozen orbital term (BS-FRZ). In Table 2, the BS-FRZ term is compared against

the spin-pure (triplet) frozen interaction (FRZ) and the sum of FRZ+SC, which is the entire energy change associated with frozen orbitals. It is evident that the BS-FRZ values lie somewhere between FRZ and FRZ+SC. Thus, BS-FRZ captures part of the spin-coupling energy, which is not fully satisfactory. In particular, FRZ represents electrostatics and Pauli repulsion in the absence of spin coupling, where the kinetic energy delocalization stabilization described by Ruedenberg is prohibited. SC then directly measures the strength of that delocalization. By contrast BS-FRZ cannot be cleanly interpreted either way because it captures just part of SC. By implication, the orbital response term in ZR-EDA (which is subtractively determined as –152.0 and –88.3 kcal/mol for ethane and fluorine, respectively) contains the remainder of the spin coupling, plus any POL and CT effects, rendering its interpretation difficult. Our new EDA has increased detail relative to the ZR-EDA, being able to separate spin-coupling, polarization, and charge-transfer contributions, which contain a great deal of information about the nature of different bonds.

One feature of our new EDA is that, unlike some methods,<sup>45</sup> each relevant energy term is relatively similar in magnitude to the total interaction energy. By avoiding large changes in large numbers, trends can be more easily seen, as evidenced by the gradual decrease in the importance of simple spin-coupling and concomitant increase in the importance of charge-transfer in first row element–H bonds (Figure 4 and Table 3). First-row atoms are highly electronegative and not very polarizable, and so the move rightward along the first row leads principally to charge-shift bonds rather than polar covalent bonds except in the case of ammonia. One way to see this trend more clearly is to sum the frozen term and the spin-coupling term. When spin-coupling dominates the bonding (i.e., when the bond is simply covalent), the spin-coupling stabilization makes up for all of the frozen term’s destabilization and much of the bond strength. Moving to the right, spin-coupling is insufficient to solely account for both the frozen term and the bond strength. Polarization and charge-transfer effects are required, culminating in the charge-shift bonds in H<sub>2</sub>O and HF where the spin-coupling cannot even fully overcome the frozen destabilization. Of course, this is not to say that spin-coupling is unimportant in these molecules; this FRZ+SC way of looking at the bond is biased against spin-coupling by forcing that term alone to account for all of the frozen destabilization, but it is a convenient way to investigate trends among the three main bonding contributors.

The EDA as bonds are broken also lends insight into the nature of the bonded interaction. By inspection of the H<sub>2</sub> EDA of dissociation (Figure 5a), one can see that the bonding in H<sub>2</sub> is dominated by spin-coupling everywhere on the potential curve. In contrast, the bond in HF (Figure 5b) at shorter bond lengths (near equilibrium) has higher spin-coupling than charge-transfer, but as the bond is stretched charge-transfer becomes relatively more important and spin-coupling and charge-transfer are about equal in magnitude. In other words, while the spin-coupling decays as the bond is stretched, the slower to decay ionic stabilization due to charge-transfer keeps the bond from weakening as much. This observation is reflective of the oft-cited fact that ionic contributions are important to understanding the strong bond in HF and that the dipole moment for HF increases as the bond is stretched.

The EDA can be used to study environmental effects on bonded interactions as well. Solvation can play a huge role in

**Table 2. Comparison of Frozen Interactions in Broken-Symmetry and Spin-Pure EDA<sup>a</sup>**

	FRZ	FRZ+SC	BS-FRZ	BS-S <sup>2</sup>
H <sub>3</sub> C–CH <sub>3</sub>	293.7	–58.0	45.0	0.585
F–F	108.5	38.2	71.9	0.959

<sup>a</sup>All energies are in kcal/mol. The broken symmetry S<sup>2</sup> value is given in the last column.

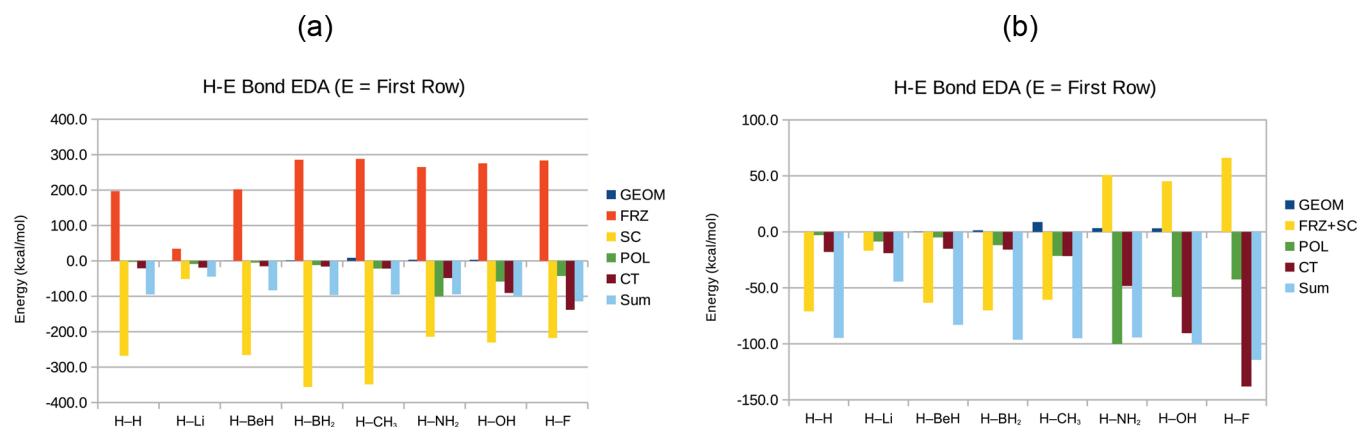


**Figure 4.** a) EDA of first row element–H bonds. Note the gradual increase in importance of charge-transfer as the element becomes more electronegative. b) EDA of first row element–H bonds with the frozen and spin-coupling terms summed to give a clearer view of the importance of different effects on a more bond-energy relevant scale.

**Table 3.** EDA of First Row Element–H Bonds<sup>a</sup>

	GEOM	FRZ	SC	POL	CT	sum	exact
H–H	0.0	196.9	–267.9 (91.9)	–2.9 (1.0)	–20.8 (7.1)	–94.7	–107.4
H–Li	0.0	34.3	–51.1 (65.0)	–8.6 (10.9)	–19.0 (24.1)	–44.4	–58.3
H–BeH	0.2	202.3	–265.6 (93.0)	–4.9 (1.7)	–15.0 (5.3)	–83.0	–97.4
H–BH <sub>2</sub>	1.4	285.7	–355.8 (92.8)	–11.8 (3.1)	–15.8 (4.1)	–96.3	–111.2
H–CH <sub>3</sub>	8.8	288.0	–348.6 (89.0)	–21.5 (5.5)	–21.6 (5.5)	–94.9	–112.2
H–NH <sub>2</sub>	3.3	265.1	–214.2 (59.1)	–100.1 (27.6)	–48.4 (13.3)	–94.3	–114.6
H–OH	3.2	275.6	–230.4 (60.8)	–58.1 (15.3)	–90.4 (23.9)	–100.2	–124.4
H–F	0.0	283.6	–217.5 (54.7)	–42.5 (10.7)	–138.0 (34.7)	–114.3	–140.1

<sup>a</sup>All energies are in kcal/mol. Numbers in parentheses are the percentage of the total stabilizing interaction energy each term represents. Exact is CCSD(T)/aug-cc-pvtz.

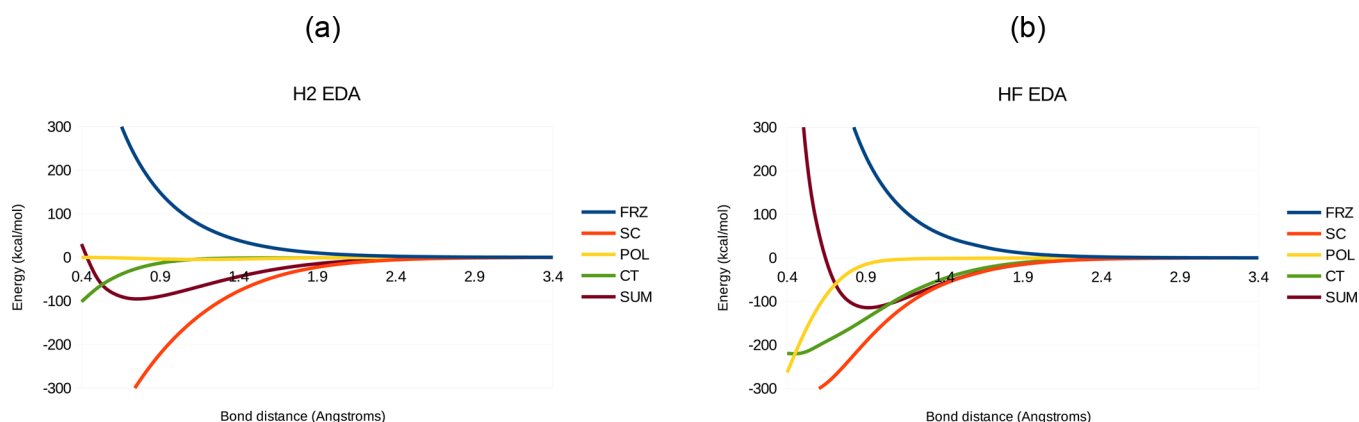


**Figure 5.** a) EDA of H<sub>2</sub> along its dissociation curve. Note that spin-coupling is dominant along the entire surface. b) EDA of HF along its dissociation curve. Note that polarization is small and the bond is dominated by spin-coupling and charge-transfer.

the nature of bonds particularly by stabilizing charge-separated states.<sup>57</sup> We investigated the effect of solvent on the HCl molecule. Experimentally, in the gas phase, HCl is a polar covalent molecule, while it dissociates into ions when dissolved in water.<sup>58</sup> Adding two explicit water molecules to HCl, one

near the H and the other near the Cl (see Figure 6a), dramatically changes the results of the EDA of the H–Cl bond (see Figure 6b). We can understand changes to the character of the bond by investigating the percentage of the total stabilizing interactions each term accounts for. Charge-transfer, a small



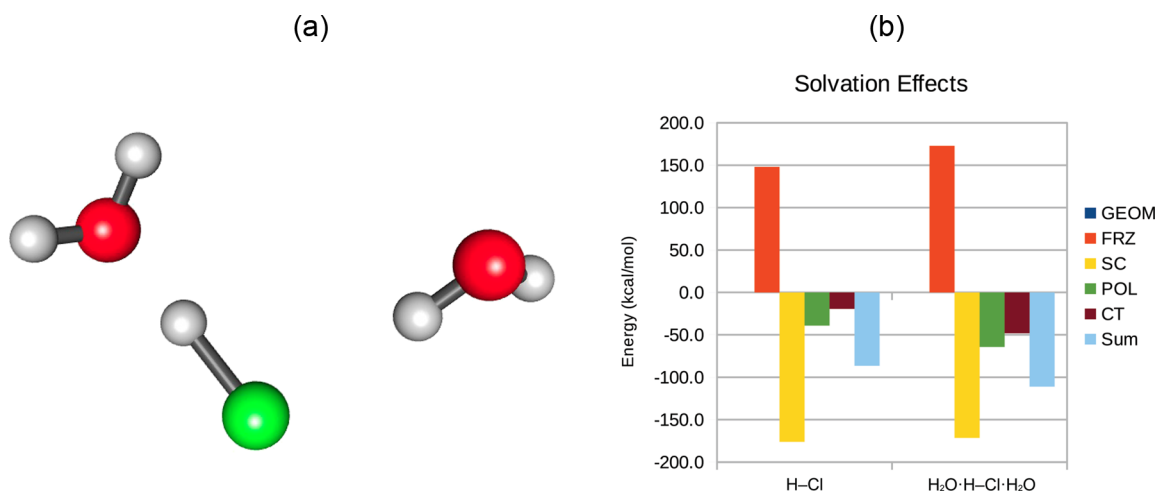


**Figure 6.** a) Solvated HCl model with two explicit water molecules. b) Effects of solvation on H-Cl bond EDA. Increase in CT and polarization indicate that the molecule becomes more ionic when solvated partially by water.

component of the gas-phase bond (8%), more than doubles in importance (17%) in the partially solvated case. Simultaneously, the polarization term increases from 17% in the gas phase to 23% in the partially solvated case. There is also a drop in the spin-coupling energy (75% to 60%). The increasing importance of the CT term and decreasing importance of spin-coupling indicates that the bond is becoming more ionic as water molecules are added. These results quantitatively describe the transformation of HCl from a polar covalent molecule to what is ultimately an ionic bond in solution as water molecules are added to the first solvation shell.

## 6. CONCLUSIONS

We have developed an extension of ALMO-EDA to single bonds in a spin-pure way, which allows the qualitatively correct bond energy to be decomposed. This method includes a new EDA term, spin-coupling, to describe the “covalency” of the bond in an energetic way. This scheme recovers chemical concepts of bonding and furthermore parametrizes these concepts quantitatively. Encouragingly, the method nicely captures differences in the character of different single bonds and, in addition, the method is sensitive to even subtle environmental changes, such as solvation.

Currently, this method is only implemented for single-bonds corresponding to the CAS(2,2) wave function; the extension to multiple-bonds may be accomplished in several ways depending on which method, such as larger CAS( $n,n$ ) expansions or stronger spin-pure approximations such as the CCVB method,<sup>59</sup> is employed to give the final interaction energy. Currently, there is also a lack of dynamical correlation in these energy terms (and thus no dispersion contribution), a problem which remains to be addressed and is currently being investigated. The promising results obtained here suggest that these extensions are worthwhile.

## AUTHOR INFORMATION

### Corresponding Author

\*E-mail: [mhg@cchem.berkeley.edu](mailto:mhg@cchem.berkeley.edu).

### Notes

The authors declare no competing financial interest.

## ACKNOWLEDGMENTS

This work was supported by a grant (CHE-1363342) from the U.S. National Science Foundation.

## REFERENCES

- (1) Pauling, L. *The Nature of the Chemical Bond and the Structure of Molecules and Crystals: An Introduction to Modern Structural Chemistry*, 3rd ed.; Cornell University Press: Ithaca, NY, 1960.
- (2) Ruedenberg, K. *Rev. Mod. Phys.* **1962**, *34*, 326–376.
- (3) Nascimento, M. A. C. *J. Braz. Chem. Soc.* **2008**, *19*, 245–256.
- (4) Kolos, W.; Wolniewicz, L. *J. Chem. Phys.* **1965**, *43*, 2429–2441.
- (5) Feinberg, M. J.; Ruedenberg, K. *J. Chem. Phys.* **1971**, *54*, 1495–1511.
- (6) Driessler, F.; Kutzelnigg, W. *Theoret. Chim. Acta* **1976**, *43*, 1–27.
- (7) Goddard, W. A., III; Wilson, C. W., Jr. *Theoret. Chim. Acta* **1972**, *26*, 211–230.
- (8) Bacskay, G. B.; Reimers, J. R.; Nordholm, S. *J. Chem. Educ.* **1997**, *74*, 1494.
- (9) Bacskay, G. B.; Nordholm, S. *J. Phys. Chem. A* **2013**, *117*, 7946–7958.
- (10) Schmidt, M. W.; Ivanic, J.; Ruedenberg, K. *J. Chem. Phys.* **2014**, *140*, 204104.
- (11) Cardozo, T. M.; Nascimento, M. A. C. *J. Chem. Phys.* **2009**, *130*, 104102.
- (12) Fantuzzi, F.; Nascimento, M. A. C. *J. Chem. Theory Comput.* **2014**, *10*, 2322–2332.
- (13) Fantuzzi, F.; Cardozo, T. M.; Nascimento, M. A. C. *J. Phys. Chem. A* **2015**, *119*, 5335–5343.
- (14) Reed, A. E.; Curtiss, L. A.; Weinhold, F. *Chem. Rev.* **1988**, *88*, 899–926.
- (15) Bader, R. F. W. *Acc. Chem. Res.* **1985**, *18*, 9–15.
- (16) Blanco, M. A.; Martín Pendás, A.; Francisco, E. *J. Chem. Theory Comput.* **2005**, *1*, 1096–1109.
- (17) Rahm, M.; Hoffmann, R. *J. Am. Chem. Soc.* **2015**, *137*, 10282–10291.
- (18) Rybak, S.; Jeziorski, B.; Szalewicz, K. *J. Chem. Phys.* **1991**, *95*, 6576–6601.
- (19) Jeziorski, B.; Moszynski, R.; Szalewicz, K. *Chem. Rev.* **1994**, *94*, 1887–1930.
- (20) Adams, W. H. *Theor. Chem. Acc.* **2002**, *108*, 225–231.
- (21) Misquitta, A. J.; Jeziorski, B.; Szalewicz, K. *Phys. Rev. Lett.* **2003**, *91*, 033201.
- (22) Misquitta, A. J.; Podeszwa, R.; Jeziorski, B.; Szalewicz, K. *J. Chem. Phys.* **2005**, *123*, 214103.
- (23) Stone, A. J.; Misquitta, A. J. *Chem. Phys. Lett.* **2009**, *473*, 201–205.



- (24) Hohenstein, E. G.; Sherrill, C. D. *WIREs Comput. Mol. Sci.* **2012**, 2, 304–326.
- (25) Lao, K. U.; Herbert, J. M. *J. Phys. Chem. Lett.* **2012**, 3, 3241–3248.
- (26) Glendening, E. D.; Streitwieser, A. *J. Chem. Phys.* **1994**, 100, 2900–2909.
- (27) Schenter, G. K.; Glendening, E. D. *J. Phys. Chem.* **1996**, 100, 17152–17156.
- (28) Glendening, E. D. *J. Phys. Chem. A* **2005**, 109, 11936–11940.
- (29) Kitaura, K.; Morokuma, K. *Int. J. Quantum Chem.* **1976**, 10, 325–340.
- (30) Ziegler, T.; Rauk, A. *Inorg. Chem.* **1979**, 18, 1755–1759.
- (31) Ziegler, T.; Rauk, A. *Inorg. Chem.* **1979**, 18, 1558–1565.
- (32) Mitoraj, M. P.; Michalak, A.; Ziegler, T. *J. Chem. Theory Comput.* **2009**, 5, 962–975.
- (33) Mo, Y.; Gao, J.; Peyerimhoff, S. D. *J. Chem. Phys.* **2000**, 112, 5530–5538.
- (34) Mo, Y.; Bao, P.; Gao, J. *Phys. Chem. Chem. Phys.* **2011**, 13, 6760.
- (35) Khaliullin, R. Z.; Head-Gordon, M.; Bell, A. T. *J. Chem. Phys.* **2006**, 124, 204105.
- (36) Khaliullin, R. Z.; Cobar, E. A.; Lochan, R. C.; Bell, A. T.; Head-Gordon, M. *J. Phys. Chem. A* **2007**, 111, 8753–8765.
- (37) Horn, P. R.; Head-Gordon, M. *J. Chem. Phys.* **2015**, 143, 114111.
- (38) Horn, P. R.; Head-Gordon, M. *J. Chem. Phys.* **2016**, 144, 084118.
- (39) Horn, P. R.; Mao, Y.; Head-Gordon, M. *J. Chem. Phys.* **2016**, 144, 114107.
- (40) Horn, P. R.; Mao, Y.; Head-Gordon, M. *Phys. Chem. Chem. Phys.* **2016**, 18, 23067–23079.
- (41) Źuchowski, P. S.; Podeszwa, R.; Moszyński, R.; Jezierski, B.; Szalewicz, K. *J. Chem. Phys.* **2008**, 129, 084101.
- (42) Hapka, M.; Źuchowski, P. S.; Szczęśniak, M. M.; Chalański, G. *J. Chem. Phys.* **2012**, 137, 164104.
- (43) Horn, P. R.; Sundstrom, E. J.; Baker, T. A.; Head-Gordon, M. *J. Chem. Phys.* **2013**, 138, 134119.
- (44) Bickelhaupt, F. M.; Baerends, E. J. In *Reviews in Computational Chemistry*; Lipkowitz, K. B., Boyd, D. B., Eds.; John Wiley & Sons, Inc.: 2000; pp 1–86.
- (45) Hopfgarten, M. v.; Frenking, G. *WIREs Comput. Mol. Sci.* **2012**, 2, 43–62.
- (46) Hendrickx, K.; Braida, B.; Bultinck, P.; Hiberty, P. C. *Comput. Theor. Chem.* **2015**, 1053, 180–188.
- (47) Roos, B. O. In *Advances in Chemical Physics*; Lawley, K. P., Ed.; John Wiley & Sons, Inc.: 1987; pp 399–445.
- (48) Hay, P. J.; Hunt, W. J.; Goddard, W. A. *J. Am. Chem. Soc.* **1972**, 94, 8293–8301.
- (49) Jensen, F. *Introduction to Computational Chemistry*, 2nd ed.; Wiley: Chichester, England; Hoboken, NJ, 2007.
- (50) Azar, R. J.; Horn, P. R.; Sundstrom, E. J.; Head-Gordon, M. *J. Chem. Phys.* **2013**, 138, 084102.
- (51) Shaik, S.; Danovich, D.; Wu, W.; Hiberty, P. C. *Nat. Chem.* **2009**, 1, 443–449.
- (52) Anderson, P.; Petit, A.; Ho, J.; Mitoraj, M. P.; Coote, M. L.; Danovich, D.; Shaik, S.; Braida, B.; Ess, D. H. *J. Org. Chem.* **2014**, 79, 9998–10001.
- (53) Zhang, H.; Danovich, D.; Wu, W.; Braida, B.; Hiberty, P. C.; Shaik, S. *J. Chem. Theory Comput.* **2014**, 10, 2410–2418.
- (54) Head-Gordon, M.; Maslen, P. E.; White, C. A. *J. Chem. Phys.* **1998**, 108, 616–625.
- (55) Shao, Y.; Gan, Z.; Epifanovsky, E.; Gilbert, A. T. B.; Wormit, M.; Kussmann, J.; Lange, A. W.; Behn, A.; Deng, J.; Feng, X.; Ghosh, D.; Goldey, M.; Horn, P. R.; Jacobson, L. D.; Kaliman, I.; Khaliullin, R. Z.; Kuś, T.; Landau, A.; Liu, J.; Proynov, E. I.; Rhee, Y. M.; Richard, R. M.; Rohrdanz, M. A.; Steele, R. P.; Sundstrom, E. J.; H. L. W., III; Zimmerman, P. M.; Zuev, D.; Albrecht, B.; Alguire, E.; Austin, B.; Beran, G. J. O.; Bernard, Y. A.; Berquist, E.; Brandhorst, K.; Bravaya, K. B.; Brown, S. T.; Casanova, D.; Chang, C.-M.; Chen, Y.; Chien, S. H.; Closser, K. D.; Crittenden, D. L.; Diedenhofen, M.; R. A. D., Jr; Do, H.; Dutoi, A. D.; Edgar, R. G.; Fatehi, S.; Fusti-Molnar, L.; Ghysels, A.; Golubeva-Zadorozhnaya, A.; Gomes, J.; Hanson-Heine, M. W. D.; Harbach, P. H. P.; Hauser, A. W.; Hohenstein, E. G.; Holden, Z. C.; Jagau, T.-C.; Ji, H.; Kaduk, B.; Khistyayev, K.; Kim, J.; Kim, J.; King, R. A.; Klunzinger, P.; Kosenkov, D.; Kowalczyk, T.; Krauter, C. M.; Lao, K. U.; Laurent, A. D.; Lawler, K. V.; Levchenko, S. V.; Lin, C. Y.; Liu, F.; Livshits, E.; Lochan, R. C.; Luenser, A.; Manohar, P.; Manzer, S. F.; Mao, S.-P.; Mardirossian, N.; Marenich, A. V.; Maurer, S. A.; Mayhall, N. J.; Neuscamman, E.; Oana, C. M.; Olivares-Amaya, R.; O'Neill, D. P.; Parkhill, J. A.; Perrine, T. M.; Peverati, R.; Prociuk, A.; Rehn, D. R.; Rosta, E.; Russ, N. J.; Sharada, S. M.; Sharma, S.; Small, D. W.; Sodt, A.; Stein, T.; Stück, D.; Su, Y.-C.; Thom, A. J. W.; Tsuchimochi, T.; Vanovschi, V.; Vogt, L.; Vydrov, O.; Wang, T.; Watson, M. A.; Wenzel, J.; White, A.; Williams, C. F.; Yang, J.; Yeganeh, S.; Yost, S. R.; You, Z.-Q.; Zhang, I. Y.; Zhang, X.; Zhao, Y.; Brooks, B. R.; Chan, G. K. L.; Chipman, D. M.; Cramer, C. J.; W. A. G., III; Gordon, M. S.; Hehre, W. J.; Klamt, A.; H. F. S., III; Schmidt, M. W.; Sherrill, C. D.; Truhlar, D. G.; Warshel, A.; Xu, X.; Aspuru-Guzik, A.; Baer, R.; Bell, A. T.; Besley, N. A.; Chai, J.-D.; Dreuw, A.; Dunietz, B. D.; Furlani, T. R.; Gwaltney, S. R.; Hsu, C.-P.; Jung, Y.; Kong, J.; Lambrecht, D. S.; Liang, W.; Ochsenfeld, C.; Rassolov, V. A.; Slipchenko, L. V.; Subotnik, J. E.; Voorhis, T. V.; Herbert, J. M.; Krylov, A. I.; Gill, P. M. W.; Head-Gordon, M.; Woodcock, H. L.; DiStasio, R. A.; Goddard, W. A.; Schaefer, H. F.; Van Voorhis, T. *Mol. Phys.* **2015**, 113, 184–215.
- (56) Kovács, A.; Esterhuysen, C.; Frenking, G. *Chem. - Eur. J.* **2005**, 11, 1813–1825.
- (57) Anslyn, E. V.; Dougherty, D. A. *Modern Physical Organic Chemistry*, 1st ed.; University Science: Sausalito, CA, 2005.
- (58) Masia, M.; Forbert, H.; Marx, D. *J. Phys. Chem. A* **2007**, 111, 12181–12191.
- (59) Small, D. W.; Lawler, K. V.; Head-Gordon, M. *J. Chem. Theory Comput.* **2014**, 10, 2027–2040.